Adjustable picometer-stable interferometers for testing space-based gravitational wave detectors

Marcel Beck[1], Shreevathsa Chalathadka Subrahmanya[1] & Oliver Gerberding[1]

[1] Institute of Experimental Physics, University of Hamburg, Luruper Chaussee 149, 22761 Hamburg, Germany

E-mail: `marcel.beck@physik.uni-hamburg.de`; `oliver.gerberding@uni-hamburg.de`

January 2025

Abstract. Space-based gravitational wave detectors, such as the Laser Interferometer Space Antenna (LISA), use picometer-precision laser interferometry to detect gravitational waves at frequencies from $1\,\mathrm{Hz}$ down to below $0.1\,\mathrm{mHz}$. Laser interferometers used for on-ground prototyping and testing of such instruments are typically constructed by permanently bonding or gluing optics onto an ultra-stable bench made of low-expansion glass ceramic. This design minimizes temperature coupling to length and tilt, which dominates the noise at low frequencies due to finite temperature stability achievable in laboratories and vacuum environments. Here, we present the study of an alternative opto-mechanical concept where optical components are placed with adjustable and freely positionable mounts on an ultra-stable bench, while maintaining picometer length stability. With this concept, a given interferometer configuration can be realised very quickly due to a simplified and speed-up assembly process, reducing the realisation time from weeks or months to a matter of hours. We built a corresponding test facility and verified the length stability of our concept by measuring the length change in an optical cavity that was probed with two different locking schemes, heterodyne laser frequency stabilisation and Pound-Drever-Hall locking. We studied the limitations of both locking schemes and verified that the cavity length noise is below $1\,\mathrm{pm}/\sqrt{\mathrm{Hz}}$ for frequencies down to $3\,\mathrm{mHz}$. We thereby demonstrate that our concept can simplify the testing of interferometer configurations and opto-mechanical components and is suitable to realise flexible optical ground support equipment for space missions that use laser interferometry, such as future space-based gravitational wave detectors and satellite geodesy missions.

Keywords: laser interferometry, gravitational wave detection, ultra-stable interferometers

1. Introduction

The Laser Interferometer Space Antenna (LISA) is a future space-based gravitational wave observatory that will measure gravitational waves (GWs) frequencies from $1\,\mathrm{Hz}$ down to below $0.1\,\mathrm{mHz}$ [10], complementary to terrestrial GW detectors at audio-band frequencies and pulsar-timings at very low frequencies [1, 2, 3]. LISA consists of three spacecrafts, each containing two test masses, forming an equilateral triangle with a distance of 2.5 million kilometers between them. When a gravitational wave passes through the detector, the relative distance between the spacecraft in which the test masses are located changes and is measured by LISA using heterodyne laser interferometry. The required displacement sensitivity within the LISA optical system, denoted by $u(f)$, in the sub-Hz regime is specified as

$$u(f) = 1\,\frac{\mathrm{pm}}{\sqrt{\mathrm{Hz}}} \times \sqrt{1 + \left(\frac{2\,\mathrm{mHz}}{f}\right)^4} \qquad \left(10^{-4}\,\mathrm{Hz} < f < 1\,\mathrm{Hz}\right). \qquad (1)$$

To achieve such low-frequency displacement sensing noise, the optical bench of LISA is going to be constructed by bonding optics onto a low-expansion glass ceramic with a small coefficient of thermal expansion (CTE) [6]. Similar approaches have been used to built optical ground support equipment (OGSE) for the mission [8, 30, 36]. The bonding process to realise such interferometers requires precise pre-alignment, extensive planning and preparation, which have motivated the study of alternative approaches to realise such interferometers for ground testing, where, for example, the robustness against mechanical vibrations of a bonded interferometer is not needed. This is further motivated by the need for testing of laser interferometers for other space-based gravitational wave detectors [14, 24], for satellite geodesy missions [23, 35], and for other uses of ultra-stable laser interferometers in areas such as dark matter searches [29, 34] and ultra-stable spectroscopy [9, 25].

We present and demonstrate a concept to realise adjustable laser interferometers satisfying the same low-frequency length stability required for LISA, where opto-mechanical components are mounted onto a low-expansion glass ceramic plate with threaded screws and clamps, similar to a typical optical table. The so-realised concept is a further development of a previously demonstrated scheme by Kulkarni *et al.* [22] where adjustable mirrors were placed on fixed points of a low-expansion baseplate. Our concept enables the fast realisation of arbitrary interferometer configurations (within the size of the given optical bench), and it allows us to reuse the setup and components for various optical experiments and thus reduce costs, for example, for OGSE. We refer to the so-prepared opto-mechanics and the corresponding testing infrastructure as toolset for adjustable picometer-stable interferometers (TAPSI).

In the initial section of this paper, we describe the opto-mechanical design of our toolset, followed by the optical test facility to shield the interferometer from external noise, especially from temperature fluctuations and mechanical vibrations. To verify the initial stability of our toolset, we set up an optical cavity and measured relative

length changes using two different locking schemes, the Heterodyne laser frequency Stabilization (HS) and the Pound-Drever-Hall (PDH) locking. Subsequently, the results and current limitations are discussed, and possible noise sources are addressed. Finally, we provide an outlook for future improvements.

2. Opto-Mechanical Concept of TAPSI

The toolset for adjustable picometer-stable interferometers (TAPSI) combines a glass ceramic optical bench with thermally compensated mirror mounts which are mounted on the bench using low thermal expansion opto-mechanics. The mirror mounts used are ZeroDrift mirror mounts from Newport with a substantially lower tilt to length coupling (TTLC) compared to standard (stainless steel) mirror mounts [27]. The opto-mechanics are made of Invar while the optical bench is made out of Zerodur . Both materials chosen have a low CTE, which is essential to reduce the critical temperature to length (and tilt) coupling at low frequencies.

The posts supporting the mirror mounts are fixed onto the bench with clamps and secured with screws and locknuts. An additional compensation plate is located between the mount and the post, so that the mounting concept is designed in such a way that the center of the mirror is above the post (see figure 1). This configuration allows for the expansion and contraction of the mirror mount and the Invar compensation plate to cancel each other out. The CTE of the thermally compensated mirror mounts was unknown but expected to be small due to the quoted low levels of beam tilts during thermal cycling. Consequently we decided to use Invar for the compensation plate, as it has one of the smallest CTEs. A future study could investigate the exact CTE of the ZeroDrift mirror mounts to further optimise the length and material of the compensation plate.

(a) Setup of the prototype cavity   (b) Side view of the mounting concept
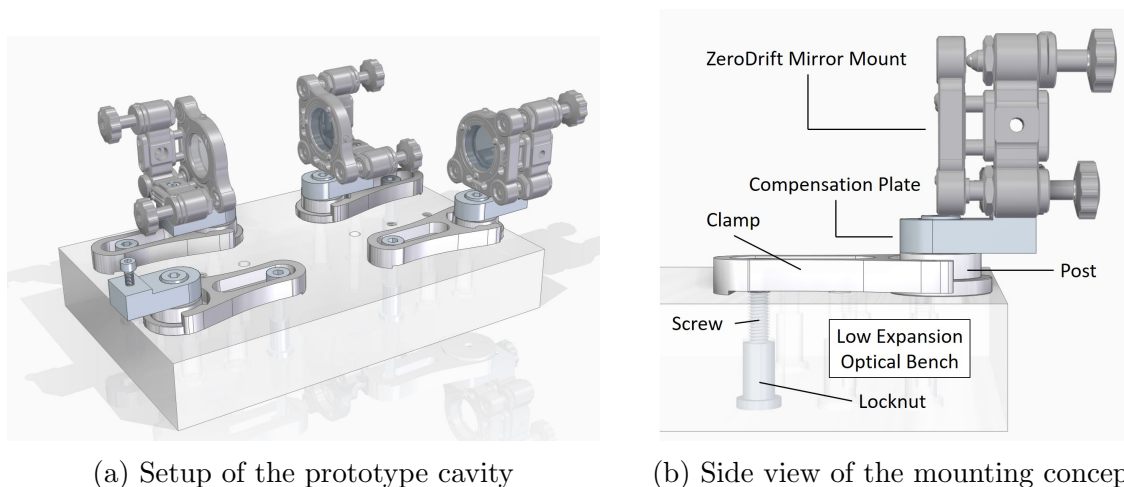
Figure 1: CAD model of the toolset for adjustable picometer-stable interferometers (TAPSI) assembly concept and the corresponding setup of the prototype cavity for measuring and verifying the length stability in section 4.

3. Test Facility

The test facility hosts the optical toolset and consists of a vacuum chamber and multiple thermal shields. The outer thermal shield consists of a Styrodur insulation that houses the vacuum chamber. The double-layer inner thermal shield is made of aluminium and is additionally covered with a multi-layer insulation foil. PEEK spacers isolate the chamber, the thermal shield, and the central aluminium breadboard from direct thermal conduction while carrying the corresponding part of the setup. The optical bench, made of Zerodur, rests on the aluminium breadboard by its own weight. A vertical cross-sectional view of the setup is shown in figure 2.

The test facility is located below a laminar flow box inside a temperature and humidity controlled laboratory. For the experiments discussed in this paper, we used a scroll pump that provides an equilibrium vacuum of 10^{-3} mbar. The vacuum chamber has an additional flange at the bottom, dedicated to directly host a turbo pump. This provision can be used in future experiments to achieve higher vacuum levels, if needed.
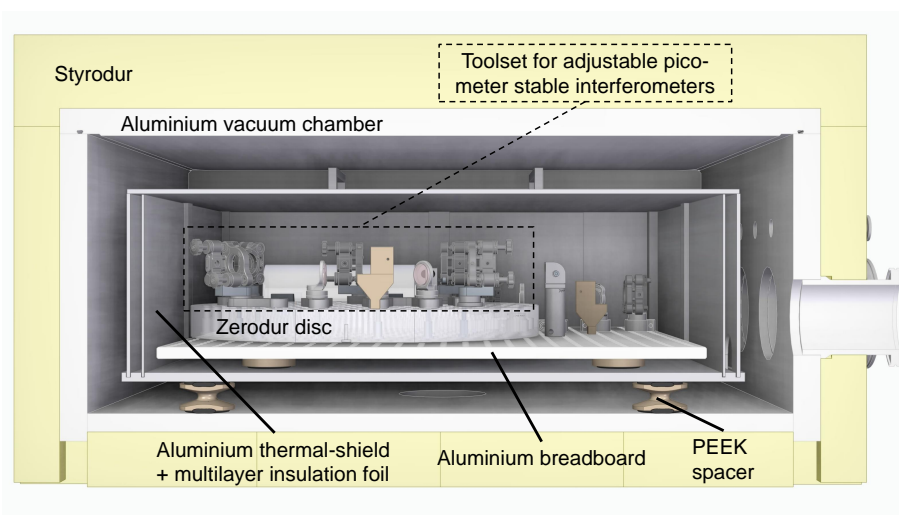

Figure 2: Vertical cross-sectional view of the optical test facility with the toolset for adjustable picometer-stable interferometers (TAPSI) inside. A pressure level of 10^{-3} mbar inside the vacuum chamber, multiple thermal isolation layers, and PEEK spacers significantly reduce temperature coupling, which is crucial at low frequencies.

In order to monitor the temperature fluctuations inside the vacuum chamber, a temperature sensor was developed. The sensor is based on the Wheatstone bridge principle and utilises a negative temperature coefficient (NTC) resistor. The design is based on previous works on temperature sensors for LISA [31, 32, 11]. The sensor was located in close proximity to the toolset and the cavity under test in section 4. Representative temperature measurements are plotted in figure 3 and the corresponding spectra in figure 4, together with the temperature of the air flow onto the chamber measured with an additional sensor. Inside the chamber, where the interferometer

toolset is placed, a temperature stability of $10\,\mu\mathrm{K}/\sqrt{\mathrm{Hz}}$ down to $10\,\mathrm{mHz}$ was achieved. The theoretical achievable sensitivity is limited by the Johnsen-Nyquist noise of the Wheatstone bridge resistors ($50\,\mathrm{k}\Omega$, $85\,\mathrm{k}\Omega$) and the NTC sensor ($85\,\mathrm{k}\Omega$) [17, 28]. The time series plot shows no direct temperature coupling between the outside and inside of the chamber, confirming the high degree of thermal isolation of our test facility. The photo-detectors (PDs) inside the chamber were identified as the source of the observed linear increase in temperature. The issue is addressed and discussed in more detail in section 5.
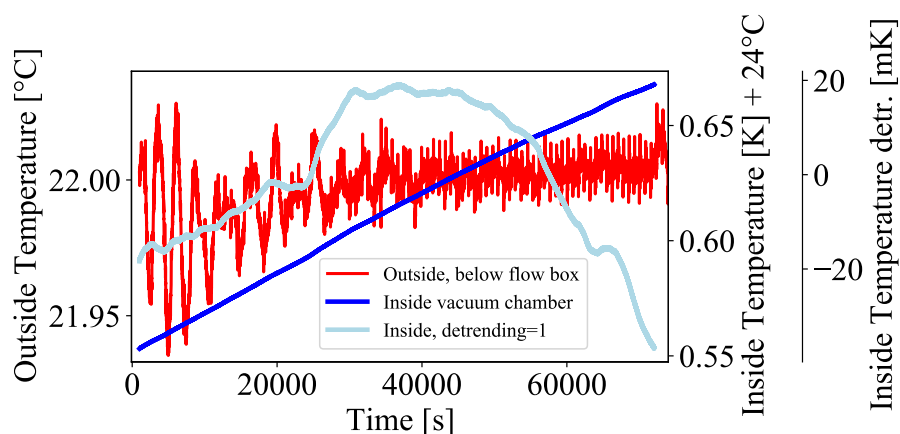

Figure 3: Time series of two parallel measurements of temperature inside and outside of the vacuum chamber. The measurement inside the chamber is also shown after subtracting the dominating linear trend caused by the heating of the PDs.
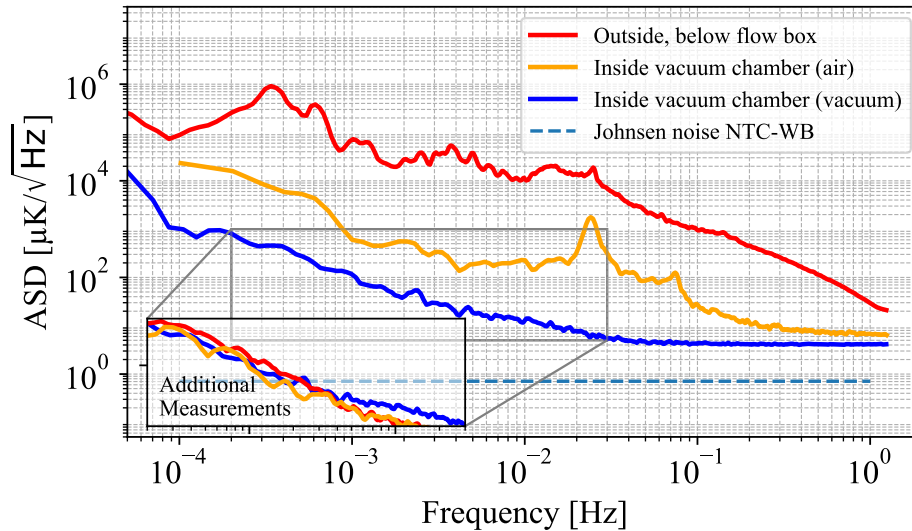
Figure 4: ASD plot (calculated with LPSD [38] after removing the linear trend from the measured time series) of the temperature outside and inside the vacuum chamber. The measurements inside the chamber were done before (air) and after reaching vacuum pressure. Additional temperature measurements were taken in conjunction with the stability measurements (figure 7) outlined in section 5. The theoretical sensitivity is given by the Johnsen-Nyquist noise of the Wheatstone bridge resistors.

4. Laser Frequency Locking

To verify the length stability of our mounting concept, we locked one of our NPRO-lasers (1064 nm) to a prototype cavity with a finesse of 627 and a length of 10 cm which was set up using the TAPSI concept (see figure 1), while the second laser was locked to a reference cavity which was constructed from an **ULE!** glass, a finesse of 10 060 and a length of 21 cm. Previous measurements of the reference cavity have demonstrated a stability of $7.5\,\mathrm{fm}/\sqrt{\mathrm{Hz}}$ ($20\,\mathrm{Hz}\sqrt{\mathrm{Hz}}$) down to 3 mHz [37]. The relative length fluctuation between the two cavities is measured by observing the change in beat-frequency of the two locked lasers. This relative length fluctuation ∂L is assumed to be dominated by the length stability of the prototype cavity and is calculated using the following relation

$$\partial L = \frac{\partial \nu}{\nu} \cdot L \tag{2}$$

where $L = 10\,\mathrm{cm}$ is the length of the prototype cavity, $\nu = 282\,\mathrm{THz}$ is the laser frequency, and $\partial \nu$ is fluctuation of the beat-frequency.

We measured the length stability of the prototype cavity using two different locking-schemes, Heterodyne laser frequency Stabilization (HS) [12] and the well-known Pound-Drever-Hall (PDH) locking [5]. Both techniques are quite similar and lock the laser's frequency to the resonance of the cavity by utilising the interaction phase shift of the cavity's reflected light. The key difference between HS and PDH locking is the method to obtain the to-be-stabilised carrier field. While PDH locking utilises sidebands which

generate an amplitude modulation from a phase modulation with the cavity interaction, HS is making use of the already existing beat-note in a heterodyne interferometer. Subsequent demodulation is performed with the sideband modulation frequency in PDH locking and with the heterodyne beat-note in HS.

4.1. Monochromatic Beam Reflection and Cavity Interaction Phase

The electric field of an incident beam can be written as

$$E_{inc} = E_0 e^{-i\omega t}, \tag{3}$$

and the reflected beam as

$$E_{refl} = E_1 e^{-i\omega t}, \tag{4}$$

where ω is the (angular) frequency and E_0, E_1 are the complex amplitudes, describing the relative phase between the two beams. The ratio of these two beams defines the reflection coefficient

$$F(\nu) = E_{refl}/E_{inc} = \frac{r_1 - r_2 e^{i2\pi \frac{\nu}{\text{FSR}}}}{1 - r_1 r_2 e^{i2\pi \frac{\nu}{\text{FSR}}}}, \tag{5}$$

where r is the amplitude reflection coefficient of each cavity mirror and $\nu = \omega/2\pi$ is the frequency of the laser light. The free spectral range $(\text{FSR}) = c/2L$ with L as the optical length of the cavity and c as the speed of light.

Far off resonance, the reflection amplitude is approximately equal to one while the phase remains constant $(F(\nu) \approx 1)$. In close proximity to the resonance, well within the line width $(\Delta\nu << \delta\nu = \nu - \nu_{res})$, the reflection coefficient is

$$F(\delta\nu) \approx \frac{r_1 - r_2}{1 - r_1 r_2} - 2\pi i \frac{r_2(1 - r_1^2)}{(1 - r_1 r_2)^2} \frac{\delta\nu}{\text{FSR}}. \tag{6}$$

For high-finesse cavities the imaginary part of the above equation can be rewritten as

$$\mathcal{I}\{F(\delta\nu)\} \approx -\mathcal{G} \frac{\delta\nu}{\Delta\nu} \tag{7}$$

with $\mathcal{G}$ summarizing the constants as an optical gain. The resulting equation (7) is linear with respect to a frequency change close to resonance. A slight deviation from the resonance of the reflected beam leads to a phase shift caused by the cavity which is proportional to the change in the length of the cavity itself.

To obtain the phase ($\propto$ length) variation information, the incident beam and the reflected beam from the cavity are measured with a PD and subsequently demodulated. This involves mixing and low-pass filtering of the two signals. The resulting so-called error-signal is used to eventually lock the laser's frequency to the resonance of the cavity. Thus, a change of the laser frequency is directly related to a change in the length of the cavity.

At this point, it is imperative to reiterate the distinction between the two locking techniques. While HS demodulates the cavity's reflected beam using the already existing heterodyne beat-note, PDH locking is using the previously generated sidebands. Each locking technique has its own set of advantages and disadvantages, which are discussed in more detail in the following subsections.

4.2. Heterodyne Laser Frequency Stabilization

The initial attempt to probe the length stability of the prototype cavity was performed with Heterodyne laser frequency Stabilization (HS) which was described and demonstrated before by Eichholz *et. al* [12]. The advantage over PDH locking is the simplicity of the locking scheme. HS utilises the existing beat-note in a heterodyne interferometer, such as LISA, and does not require phase modulators and therefore avoids their noise contribution.

The Heterodyne laser frequency Stabilization scheme is shown in figure 5. The interference signal (beat-note) was measured by PD1 and also forwarded through a polarization-maintaining, single-mode fiber into the vacuum chamber and onto the cavities. The cavity reflections were detected by PD2 and PD3, respectively, using fiber-circulators. The measured signals, consisting of the initial beat and the reflected beats from the cavities, were demodulated by analogue mixing and low-pass filtering. With additional phase shifters in front of each mixer, the phase difference was adjusted. The resulting error-signal was forwarded to a PI-controller to lock both lasers to their respective cavities.

The measurement of the PD1 beat-note converted to an amplitude spectral density (ASD) plot is showing the length stability of the prototype cavity realised with our concept TAPSI (see figure 7). After the first commissioning, we made a number of improvements, including thermal isolation of the optical fibers and electronics of the control loop.

Ultimately, we encountered an implementation limitation that is likely caused by a delay, which we refer to as *delay-beat*. The problem occurs when there is a discrepancy in the path length between the two signals, beginning from the point of interference and ending at the stage of demodulation. This includes the laser's free space propagation, the optical fiber and the electrical cable length. For example: a linear scan of the laser frequency leads to a linear change in the heterodyne frequency (beat-note). Due to the differing path lengths, the two signals will arrive at the mixer at different times, with different frequencies, resulting in a phase shift between them. This linear phase shift over time leads to an additional beat, the delay-beat.

Since we used a purely analogue demodulation, a compensation of the delay with an additional electrical cable length was only possible up to a certain degree. Furthermore, long-term frequency drifts will inevitably give rise to issues unless they are actively regulated. This problem has already been described and overcome in [12, 7] by introducing a frequency-dependent phase offset in the digital domain. However, the current experimental approach of long-term stability and the noise floor are constrained by the analogue HS. The planned transition to digital demodulation will be implemented in future experiments.

PDH locking does not encounter the problem of the *delay-beat* because the demodulation frequency, given by the electro-optic modulators (EOMs), is constant.
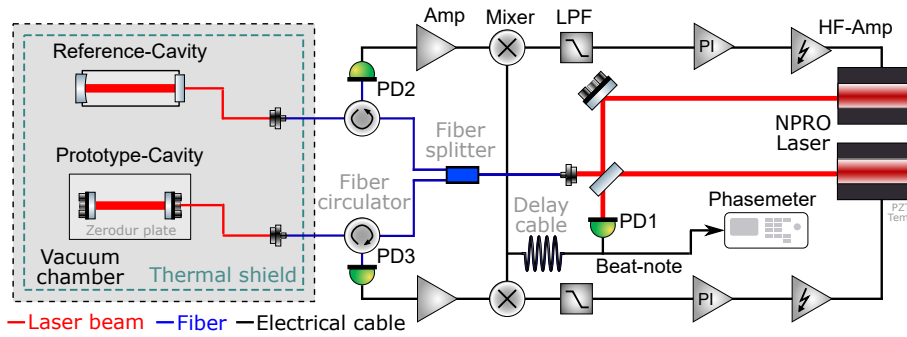
Figure 5: The Heterodyne laser frequency Stabilization scheme uses the beat-note from a heterodyne interferometer. The reflected beat-note (as detected by PD2 and PD3) is then demodulated with the initial beat-note (detected by PD1) to extract the cavity interaction phase and create an error-signal. That signal is used to lock each laser to its respective cavity. The measured beat-note by PD1 provides the information about the change in relative length of the cavities.

4.3. Pound-Drever-Hall Locking

As the actual length stability of our prototype cavity, and hence the concept, was not fully probed using the analogue HS technique, we switched to the well-known PDH locking for that purpose. The final experimental setup is shown in figure 6a). The optical setup required for PDH, including the prototype cavity, were assembled with TAPSI (see figure 6b). We were able to complete the initial placement and rough alignment of the optics in less than an hour, demonstrating the desired speed for setting up such interferometers.

From the initial commissioning phase, improvements were made to the configuration, such as the transition from fiber circulators to free space, to mitigate the anticipated stray light from the etalon effect of fiber-to-fiber connections.

We also placed the fiber-coupled EOMs within the vacuum chamber to minimize the residual amplitude modulation (RAM) [19, 20, 15]. A further challenge associated with EOMs is the misalignment of the input polarization, which results in an oscillatory rotation of the output polarization. This is subsequently converted to an amplitude modulation, for instance, by a polarization beam splitter. The EOMs we were using are based on an annealed proton-exchanged (APE) waveguide technology whereby only the transverse electrical (TE) mode is guided [26]. Any misalignment of the input polarization results in a static increase in insertion loss. Consequently, our phase modulators served the function of polarization filters as is done in standard practice of RAM suppression. The signal for the laser light modulation as well as the demodulation, error-signal and PI-controller were done by the multi-instrument mode of one Moku:Pro.

(a) PDH locking scheme
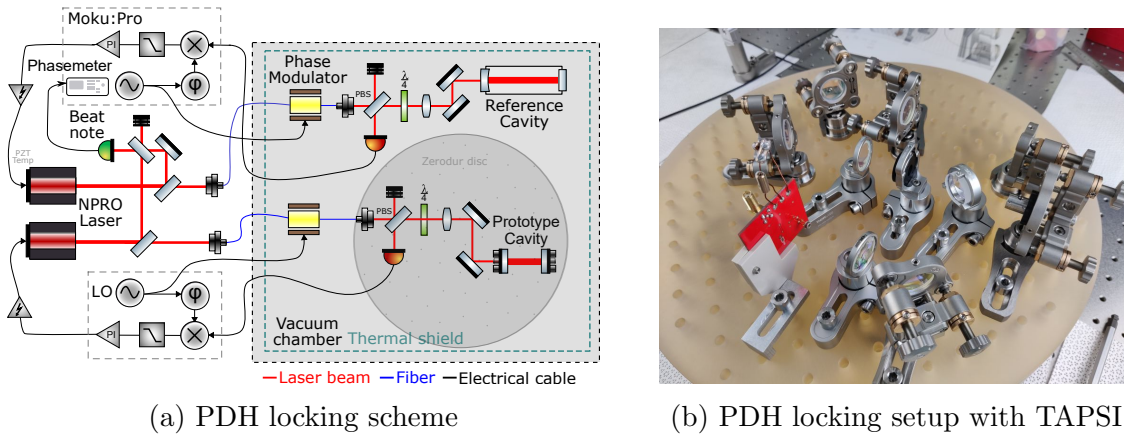

(b) PDH locking setup with TAPSI

Figure 6: (a) PDH locking scheme with fiber-coupled EOMs and free space setup inside the vacuum chamber. The beat-note provides the information about the change in relative length of the cavities and was measured with the phasemeter of the Moku:Pro. (b) Initial placement and alignment of the optics for the PDH locking was completed in less than an hour using the toolset for adjustable picometer-stable interferometers (TAPSI).

5. Results

The length stability of the adjustable picometer-stable interferometer concept was determined by measuring the length change of a prototype cavity, in comparison to an ultra-stable reference cavity. We have used two different locking schemes, the Heterodyne laser frequency Stabilization (section 4.2) and Pound-Drever-Hall locking (section 4.3). The results are shown in figure 7. Although both results of the locking schemes were improved by thermal isolation, the HS was ultimately limited by analogue demodulation. The PDH locking scheme, which was setup with the TAPSI concept in free space, is below the LISA requirements for most frequencies and only slightly above at 0.8 to 3 mHz, demonstrating the achievable length stability of our concept.

The initial PDH configuration, in which the PDs were placed outside the chamber (see the light blue trace in figure 7), revealed the presence of a typical stray light shoulder in the spectrum [13, 33]. The necessity for additional fiber components in this configuration gave rise to an increased number of fiber-to-fiber connections, leading to the formation of etalons and possibly causing parasitic beams. Furthermore, the initial configuration has incorporated fiber circulators, which have been demonstrated to induce RAM [16]. The best results of the PDH locking were achieved by using free space optics as much as possible (see figure 6a).

Although the PDH locking achieves the desired performance, a linear drift in frequency is observed and can be attributed to the linear temperature increase resulting from the PDs situated in vacuum. The variation in length per degree of temperature
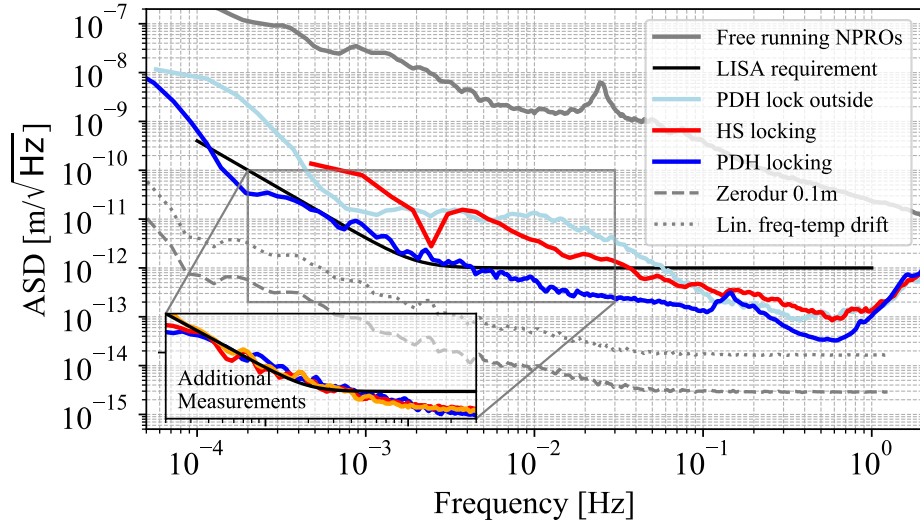
Figure 7: The length stability of the prototype cavity was measured with the Heterodyne laser frequency Stabilization (HS) and the Pound-Drever-Hall (PDH) locking techniques. Additional measurements performed with PDH locking are plotted in conjunction with temperature measurements from figure 4, highlighting the presence of non-stationary noise. In addition, the free-running laser noise of a 10 cm cavity and the theoretical length deviation of the Zerodur bench in the corresponding environment is presented.
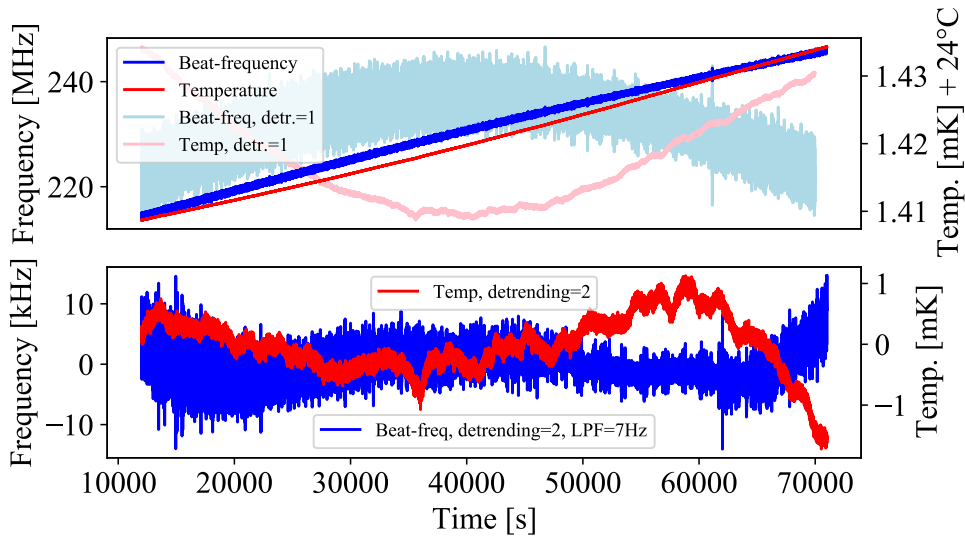

Figure 8: The upper subplot shows the time series of parallel measurements of the beat-frequency and the temperature, along with their respective subtraction of the linear drift. In the lower subplot the quadratic drift was removed, while an additional low-pass filter with a cut-off frequency of 7 Hz was applied to highlight the presence of non-stationary noise such as parasitic beams.

change can be determined from figure 8 as

$$\frac{dL}{dT} = \frac{df}{f_{Laser}} L_{Cavity} \cdot \frac{1}{dT} \approx 4 \times 10^{-8}\,\mathrm{m/K} \tag{8}$$

where df is the linear rise of the beat-frequency, f the laser frequency, L_{Cavity} the length of the prototype cavity and dT the linear rise of the temperature. The multiplication of this drift and the temperature inside the chamber (figure 4) provides insight into the linear frequency-temperature dependence. The resulting plot (see figure 7) demonstrates that the stability is not limited by this linear temperature coupling, as the projected noise lies below the length stability measurements for all frequencies. Furthermore, we confirmed that there is no discernible correlation or coherence between fluctuations in temperature and length.

The lower subplot of figure 8 shows the beat-frequency time series, after the removal of the quadratic drift and the application of a low-pass filter with a cut-off frequency of 7 Hz. The plot reveals the presence of non-stationary noise. The additional length measurements in figure 7 and the additional temperature measurements from figure 4 which were carried out in parallel, highlighting these assumptions. This phenomenon, which may be attributed to factors such as parasitic beams, could potentially explain the observed limitation in our measurement.

The geometrical tilt to length coupling of our prototype cavity (0.1 m), calculated from the ZeroDrift mirror mounts and our temperature measurement inside the chamber is below 8×10^{-13} m/K and can be excluded as a limitation. The theoretical minimum length noise of our length stability experiment is defined by the expansion of the optical bench within the length of the prototype cavity. The CTE of the Zerodur material, when multiplied with the temperature noise inside the test facility, yields the minimum length noise and is also plotted in figure 7.

6. Conclusion and Outlook

We have developed a toolset for adjustable picometer-stable interferometers (TAPSI) and shown a length stability which satisfies a $1 \, \mathrm{pm}/\sqrt{\mathrm{Hz}}$ LISA requirement for OGSE. The length measurements were performed with Heterodyne laser frequency Stabilization and PDH locking in an optical test facility with a temperature stability of 10 μK down to 10 mHz. The current noise limitations of the analogue HS is expected to be addressed in future work by moving from analogue to digital demodulation. The PDH locking scheme was completely setup with TAPSI and the initial alignment was achieved in less than an hour. Subsequent measurements have shown performance satisfying LISA requirements and demonstrating the stability of our toolset. Temperature couplings have not been identified as the predominant limitation; instead, we suspect that other noise sources associated with readout and probably stray light are the main factors limiting performance. The latter limitation could potentially be reduced with a higher finesse in the prototype cavity.

However, further improvements of the test facility are planned for future iterations, including additional thermal shielding and improvements of the temperature sensor to allow monitoring of temperature changes in the lower μK-regime. In addition, the temperature coupling of the opto-mechanical concept is also to be reduced by

replacing the toolset's compensating plate with a CTE-compliant material to match the expansion of the ZeroDrift mirror mounts. An additional improvement, which has already been demonstrated in other PDH locking experiments [21], can be achieved through monitoring RAM noise, which can be subtracted in post-processing.

In this paper, we demonstrated that glass-ceramic low-expansion optical benches in corresponding environments can be used to realise adjustable picometer-stable interferometers with flexible component placement. Although this concept can be employed to develop OGSE for LISA, it can also be used for future low-frequency space-based gravitational wave detectors such as Beyond-LISA, Taiji and DECIGO [4, 14, 18].

Data availability statement

All data that support the findings of this study are included within the article (and any supplementary files).

Acknowledgement

List of Abbreviations

TAPSI toolset for adjustable picometer-stable interferometers

LISA Laser Interferometer Space Antenna

GW gravitational wave

OGSE optical ground support equipment

HS Heterodyne laser frequency Stabilization

PDH Pound-Drever-Hall

CTE coefficient of thermal expansion

TTLC tilt to length coupling

ASD amplitude spectral density

FSR free spectral range

EOM electro-optic modulator

RAM residual amplitude modulation

PD photo-detector

ASD amplitude spectral density

APE annealed proton-exchanged

TE transverse electrical

PEEK Polyether ether ketone

NTC negative temperature coefficient

LPSD linear power spectral density

References

[1] J Aasi, B P Abbott, R Abbott, T Abbott, M R Abernathy, K Ackley, C Adams, T Adams, P Addesso, R X Adhikari, V Adya, C Affeldt, N Aggarwal, O D Aguiar, A Ain, P Ajith, A Alemic, B Allen, D Amariutei, S B Anderson, W G Anderson, K Arai, M C Araya, C Arceneaux, J S Areeda, G Ashton, S Ast, S M Aston, P Aufmuth, C Aulbert, B E Aylott, S Babak, P T Baker, S W Ballmer, J C Barayoga, M Barbet, S Barclay, B C Barish, D Barker, B Barr, L Barsotti, J Bartlett, M A Barton, I Bartos, R Bassiri, J C Batch, C Baune, B Behnke, A S Bell, C Bell, M Benacquista, J Bergman, G Bergmann, C P L Berry, J Betzwieser, S Bhagwat, R Bhandare, I A Bilenko, G Billingsley, J Birch, S Biscans, C Biwer, J K Blackburn, L Blackburn, C D Blair, D Blair, O Bock, T P Bodiya, P Bojtos, C Bond, R Bork, M Born, Sukanta Bose, P R Brady, V B Braginsky, J E Brau, D O Bridges, M Brinkmann, A F Brooks, D A Brown, D D Brown, N M Brown, S Buchman, A Buikema, A Buonanno, L Cadonati, J Calderón Bustillo, J B Camp, K C Cannon, J Cao, C D Capano, S Caride, S Caudill, M Cavaglià, C Cepeda, R Chakraborty, T Chalermsongsak, S J Chamberlin, S Chao, P Charlton, Y Chen, H S Cho, M Cho, J H Chow, N Christensen, Q Chu, S Chung, G Ciani, F Clara, J A Clark, C Collette, L Cominsky, M Constancio, D Cook, T R Corbitt, N Cornish, A Corsi, C A Costa, M W Coughlin, S Countryman, P Couvares, D M Coward, M J Cowart, D C Coyne, R Coyne, K Craig, J D E Creighton, T D Creighton, J Cripe, S G Crowder, A Cumming, L Cunningham, C Cutler, K Dahl, T Dal Canton, M Damjanic, S L Danilishin, K Danzmann, L Dartez, I Dave, H Daveloza, G S Davies, E J Daw, D DeBra, W Del Pozzo, T Denker, T Dent, V Dergachev, R T DeRosa, R DeSalvo, S Dhurandhar, M D´ıaz, I Di Palma, G Dojcinoski, E Dominguez, F Donovan, K L Dooley, S Doravari, R Douglas, T P Downes, J C Driggers, Z Du, S Dwyer, T Eberle, T Edo, M Edwards, M Edwards, A Effler, H.-B Eggenstein, P Ehrens, J Eichholz, S S Eikenberry, R Essick, T Etzel, M Evans, T Evans, M Factourovich, S Fairhurst, X Fan, Q Fang, B Farr, W M Farr, M Favata, M Fays, H Fehrmann, M M Fejer, D Feldbaum, E C Ferreira, R P Fisher, Z Frei, A Freise, R Frey, T T Fricke, P Fritschel, V V Frolov, S Fuentes-Tapia, P Fulda, M Fyffe, J R Gair, S Gaonkar, N Gehrels, L Á Gergely´, J A Giaime, K D Giardina, J Gleason, E Goetz, R Goetz, L Gondan, G González, N Gordon, M L Gorodetsky, S Gossan, S Goßler, C Gräf, P B Graff, A Grant, S Gras, C Gray, R J S Greenhalgh, A M Gretarsson, H Grote, S Grunewald, C J Guido, X Guo, K Gushwa, E K Gustafson, R Gustafson, J Hacker, E D Hall, G Hammond, M Hanke, J Hanks, C Hanna, M D Hannam, J Hanson, T Hardwick, G M Harry, I W Harry, M Hart, M T Hartman, C-J Haster, K Haughian, S Hee, M Heintze, G Heinzel, M Hendry, I S Heng, A W Heptonstall, M Heurs, M Hewitson, S Hild, D Hoak, K A Hodge, S E Hollitt, K Holt, P Hopkins, D J Hosken, J Hough, E Houston, E J Howell, Y M Hu, E Huerta, B Hughey, S Husa, S H Huttner, M Huynh, T Huynh-Dinh, A Idrisy, N Indik, D R Ingram, R Inta, G Islas, J C Isler, T Isogai, B R Iyer, K Izumi, M Jacobson, H Jang, S Jawahar, Y Ji, F Jiménez-Forteza, W W Johnson, D I Jones, R Jones, L Ju, K Haris, V Kalogera, S Kandhasamy, G Kang, J B Kanner, E Katsavounidis, W Katzman, H Kaufer, S Kaufer, T Kaur, K Kawabe, F Kawazoe, G M Keiser, D Keitel, D B Kelley, W Kells, D G Keppel, J S Key, A Khalaidovski, F Y Khalili, E A Khazanov, C Kim, K Kim, N G Kim, N Kim, Y.-M Kim, E J King, P J King, D L Kinzel, J S Kissel, S Klimenko, J Kline, S Koehlenbeck, K Kokeyama, V Kondrashov, M Korobko, W Z Korth, D B Kozak, V Kringel, B Krishnan, C Krueger, G Kuehn, A Kumar, P Kumar, L Kuo, M Landry, B Lantz, S Larson, P D Lasky, A Lazzarini, C Lazzaro, J Le, P Leaci, S Leavey, E O Lebigot, C H Lee, H K Lee, H M Lee, J R Leong, Y Levin, B Levine, J Lewis, T G F Li, K Libbrecht, A Libson, A C Lin, T B Littenberg, N A Lockerbie, V Lockett, J Logue, A L Lombardi, M Lormand, J Lough, M J Lubinski, H Lück, A P Lundgren, R Lynch, Y Ma, J Macarthur, T MacDonald, B Machenschalk, M MacInnis, D M Macleod, F Magaña-Sandoval, R Magee, M Mageswaran, C Maglione, K Mailand, I Mandel, V Mandic, V Mangano, G L Mansell, S Márka, Z Márka, A Markosyan, E Maros, I W Martin, R M Martin, D Martynov, J N Marx, K Mason, T J

Massinger, F Matichard, L Matone, N Mavalvala, N Mazumder, G Mazzolo, R McCarthy, D E McClelland, S McCormick, S C McGuire, G McIntyre, J McIver, K McLin, S McWilliams, G D Meadors, M Meinders, A Melatos, G Mendell, R A Mercer, S Meshkov, C Messenger, P M Meyers, H Miao, H Middleton, E E Mikhailov, A Miller, J Miller, M Millhouse, J Ming, S Mirshekari, C Mishra, S Mitra, V P Mitrofanov, G Mitselmakher, R Mittleman, B Moe, S D Mohanty, S R P Mohapatra, B Moore, D Moraru, G Moreno, S R Morriss, K Mossavi, C M Mow-Lowry, C L Mueller, G Mueller, S Mukherjee, A Mullavey, J Munch, D Murphy, P G Murray, A Mytidis, T Nash, R K Nayak, V Necula, K Nedkova, G Newton, T Nguyen, A B Nielsen, S Nissanke, A H Nitz, D Nolting, M E N Normandin, L K Nuttall, E Ochsner, J O'Dell, E Oelker, G H Ogin, J J Oh, S H Oh, F Ohme, P Oppermann, R Oram, B O'Reilly, W Ortega, R O'Shaughnessy, C Osthelder, C D Ott, D J Ottaway, R S Ottens, H Overmier, B J Owen, C Padilla, A Pai, S Pai, O Palashov, A Pal-Singh, H Pan, C Pankow, F Pannarale, B C Pant, M A Papa, H Paris, Z Patrick, M Pedraza, L Pekowsky, A Pele, S Penn, A Perreca, M Phelps, V Pierro, I M Pinto, M Pitkin, J Poeld, A Post, A Poteomkin, J Powell, J Prasad, V Predoi, S Premachandra, T Prestegard, L R Price, M Principe, S Privitera, R Prix, L Prokhorov, O Puncken, M Pürrer, J Qin, V Quetschke, E Quintero, G Quiroga, R Quitzow-James, F J Raab, D S Rabeling, H Radkins, P Raffai, S Raja, G Rajalakshmi, M Rakhmanov, K Ramirez, V Raymond, C M Reed, S Reid, D H Reitze, O Reula, K Riles, N A Robertson, R Robie, J G Rollins, V Roma, J D Romano, G Romanov, J H Romie, S Rowan, A Rüdiger, K Ryan, S Sachdev, T Sadecki, L Sadeghian, M Saleem, F Salemi, L Sammut, V Sandberg, J R Sanders, V Sannibale, I Santiago-Prieto, B S Sathyaprakash, P R Saulson, R Savage, A Sawadsky, J Scheuer, R Schilling, P Schmidt, R Schnabel, R M S Schofield, E Schreiber, D Schuette, B F Schutz, J Scott, S M Scott, D Sellers, A S Sengupta, A Sergeev, G Serna, A Sevigny, D A Shaddock, M S Shahriar, M Shaltev, Z Shao, B Shapiro, P Shawhan, D H Shoemaker, T L Sidery, X Siemens, D Sigg, A D Silva, D Simakov, A Singer, L Singer, R Singh, A M Sintes, B J J Slagmolen, J R Smith, M R Smith, R J E Smith, N D Smith-Lefebvre, E J Son, B Sorazu, T Souradeep, A Staley, J Stebbins, M Steinke, J Steinlechner, S Steinlechner, D Steinmeyer, B C Stephens, S Steplewski, S Stevenson, R Stone, K A Strain, S Strigin, R Sturani, A L Stuver, T Z Summerscales, P J Sutton, M Szczepanczyk, G Szeifert, D Talukder, D B Tanner, M Tápai, S P Tarabrin, A Taracchini, R Taylor, G Tellez, T Theeg, M P Thirugnanasambandam, M Thomas, P Thomas, K A Thorne, K S Thorne, E Thrane, V Tiwari, C Tomlinson, C V Torres, C I Torrie, G Traylor, M Tse, D Tshilumba, D Ugolini, C S Unnikrishnan, A L Urban, S A Usman, H Vahlbruch, G Vajente, G Valdes, M Vallisneri, A A van Veggel, S Vass, R Vaulin, A Vecchio, J Veitch, P J Veitch, K Venkateswara, R Vincent-Finley, S Vitale, T Vo, C Vorvick, W D Vousden, S P Vyatchanin, A R Wade, L Wade, M Wade, M Walker, L Wallace, S Walsh, H Wang, M Wang, X Wang, R L Ward, J Warner, M Was, B Weaver, M Weinert, A J Weinstein, R Weiss, T Welborn, L Wen, P Wessels, T Westphal, K Wette, J T Whelan, S E Whitcomb, D J White, B F Whiting, C Wilkinson, L Williams, R Williams, A R Williamson, J L Willis, B Willke, M Wimmer, W Winkler, C C Wipf, H Wittel, G Woan, J Worden, S Xie, J Yablon, I Yakushin, W Yam, H Yamamoto, C C Yancey, Q Yang, M Zanolin, Fan Zhang, L Zhang, M Zhang, Y Zhang, C Zhao, M Zhou, X J Zhu, M E Zucker, S Zuraw, and J Zweizig. Advanced ligo. *Classical and Quantum Gravity*, 32(7):074001, March 2015.

[2] F Acernese, M Agathos, K Agatsuma, D Aisa, N Allemandou, A Allocca, J Amarni, P Astone, G Balestri, G Ballardin, F Barone, J-P Baronick, M Barsuglia, A Basti, F Basti, Th S Bauer, V Bavigadda, M Bejger, M G Beker, C Belczynski, D Bersanetti, A Bertolini, M Bitossi, M A Bizouard, S Bloemen, M Blom, M Boer, G Bogaert, D Bondi, F Bondu, L Bonelli, R Bonnand, V Boschi, L Bosi, T Bouedo, C Bradaschia, M Branchesi, T Briant, A Brillet, V Brisson, T Bulik, H J Bulten, D Buskulic, C Buy, G Cagnoli, E Calloni, C Campeggi, B Canuel, F Carbognani, F Cavalier, R Cavalieri, G Cella, E Cesarini, E Chassande Mottin, A Chincarini, A Chiummo, S Chua, F Cleva, E Coccia, P-F Cohadon, A Colla, M Colombini, A Conte, J-P Coulon, E Cuoco, A Dalmaz, S D'Antonio, V Dattilo, M Davier, R Day, G Debreczeni, J Degallaix, S Deléglise,

W Del Pozzo, H Dereli, R De Rosa, L Di Fiore, A Di Lieto, A Di Virgilio, M Doets, V Dolique, M Drago, M Ducrot, G Endrőczi, V Fafone, S Farinon, I Ferrante, F Ferrini, F Fidecaro, I Fiori, R Flaminio, J-D Fournier, S Franco, S Frasca, F Frasconi, L Gammaitoni, F Garufi, M Gaspard, A Gatto, G Gemme, B Gendre, E Genin, A Gennai, S Ghosh, L Giacobone, A Giazotto, R Gouaty, M Granata, G Greco, P Groot, G M Guidi, J Harms, A Heidmann, H Heitmann, P Hello, G Hemming, E Hennes, D Hofman, P Jaranowski, R J G Jonker, M Kasprzack, F Kéfélian, I Kowalska, M Kraan, A Królak, A Kutynia, C Lazzaro, M Leonardi, N Leroy, N Letendre, T G F Li, B Lieunard, M Lorenzini, V Loriette, G Losurdo, C Magazzù, E Majorana, I Maksimovic, V Malvezzi, N Man, V Mangano, M Mantovani, F Marchesoni, F Marion, J Marque, F Martelli, L Martellini, A Masserot, D Meacher, J Meidam, F Mezzani, C Michel, L Milano, Y Minenkov, A Moggi, M Mohan, M Montani, N Morgado, B Mours, F Mul, M F Nagy, I Nardecchia, L Naticchioni, G Nelemans, I Neri, M Neri, F Nocera, E Pacaud, C Palomba, F Paoletti, A Paoli, A Pasqualetti, R Passaquieti, D Passuello, M Perciballi, S Petit, M Pichot, F Piergiovanni, G Pillant, A Piluso, L Pinard, R Poggiani, M Prijatelj, G A Prodi, M Punturo, P Puppo, D S Rabeling, I Rácz, P Rapagnani, M Razzano, V Re, T Regimbau, F Ricci, F Robinet, A Rocchi, L Rolland, R Romano, D Rosińska, P Ruggi, E Saracco, B Sassolas, F Schimmel, D Sentenac, V Sequino, S Shah, K Siellez, N Straniero, B Swinkels, M Tacca, M Tonelli, F Travasso, M Turconi, G Vajente, N van Bakel, M van Beuzekom, J F J van den Brand, C Van Den Broeck, M V van der Sluys, J van Heijningen, M Vasúth, G Vedovato, J Veitch, D Verkindt, F Vetrano, A Viceré, J-Y Vinet, G Visser, H Vocca, R Ward, M Was, L-W Wei, M Yvert, A Zadro żny, and J-P Zendri. Advanced virgo: a second-generation interferometric gravitational wave detector. *Classical and Quantum Gravity*, 32(2):024001, December 2014.

[3] Gabriella Agazie, Akash Anumarlapudi, Anne M. Archibald, Paul T. Baker, Bence Bécsy, Laura Blecha, Alexander Bonilla, Adam Brazier, Paul R. Brook, Sarah Burke-Spolaor, Rand Burnette, Robin Case, J. Andrew Casey-Clyde, Maria Charisi, Shami Chatterjee, Katerina Chatziioannou, Belinda D. Cheeseboro, Siyuan Chen, Tyler Cohen, James M. Cordes, Neil J. Cornish, Fronefield Crawford, H. Thankful Cromartie, Kathryn Crowter, Curt J. Cutler, Daniel J. D'Orazio, Megan E. DeCesar, Dallas DeGan, Paul B. Demorest, Heling Deng, Timothy Dolch, Brendan Drachler, Elizabeth C. Ferrara, William Fiore, Emmanuel Fonseca, Gabriel E. Freedman, Emiko Gardiner, Nate Garver-Daniels, Peter A. Gentile, Kyle A. Gersbach, Joseph Glaser, Deborah C. Good, Kayhan Gültekin, Jeffrey S. Hazboun, Sophie Hourihane, Kristina Islo, Ross J. Jennings, Aaron Johnson, Megan L. Jones, Andrew R. Kaiser, David L. Kaplan, Luke Zoltan Kelley, Matthew Kerr, Joey S. Key, Nima Laal, Michael T. Lam, William G. Lamb, T. Joseph W. Lazio, Natalia Lewandowska, Tyson B. Littenberg, Tingting Liu, Jing Luo, Ryan S. Lynch, Chung-Pei Ma, Dustin R. Madison, Alexander McEwen, James W. McKee, Maura A. McLaughlin, Natasha McMann, Bradley W. Meyers, Patrick M. Meyers, Chiara M. F. Mingarelli, Andrea Mitridate, Priyamvada Natarajan, Cherry Ng, David J. Nice, Stella Koch Ocker, Ken D. Olum, Timothy T. Pennucci, Benetge B. P. Perera, Polina Petrov, Nihan S. Pol, Henri A. Radovan, Scott M. Ransom, Paul S. Ray, Joseph D. Romano, Jessie C. Runnoe, Shashwat C. Sardesai, Ann Schmiedekamp, Carl Schmiedekamp, Kai Schmitz, Levi Schult, Brent J. Shapiro-Albert, Xavier Siemens, Joseph Simon, Magdalena S. Siwek, Ingrid H. Stairs, Daniel R. Stinebring, Kevin Stovall, Jerry P. Sun, Abhimanyu Susobhanan, Joseph K. Swiggum, Jacob Taylor, Stephen R. Taylor, Jacob E. Turner, Caner Unal, Michele Vallisneri, Sarah J. Vigeland, Jeremy M. Wachter, Haley M. Wahl, Qiaohong Wang, Caitlin A. Witt, David Wright, and Olivia Young. The nanograv 15 yr data set: Constraints on supermassive black hole binaries from the gravitational-wave background. *The Astrophysical Journal Letters*, 952(2):L37, August 2023.

[4] John Baker, Simon F. Barke, Peter L. Bender, Emanuele Berti, Robert Caldwell, John W. Conklin, Neil Cornish, Elizabeth C. Ferrara, Kelly Holley-Bockelmann, Brittany Kamai, Shane L. Larson, Jeff Livas, Sean T. McWilliams, Guido Mueller, Priyamvada Natarajan, Norman Rioux, Shannon R Sankar, Jeremy Schnittman, Deirdre Shoemaker, Jacob Slutsky, Robin Stebbins, Ira

Thorpe, and John Ziemer. Space based gravitational wave astronomy beyond lisa, 2019.

[5] Eric D. Black. An introduction to pound–drever–hall laser frequency stabilization. *American Journal of Physics*, 69(1):79–87, January 2001.

[6] J. Bogenstahl, C. Diekmann, E. D. Fitzsimons, R. Fleddermann, E. Granova, C. J. Killow, J. Pijnenburg, D. I. Robertson, A. Shoda, A. Sohmer, M. Tröbs, H. Ward, D. Weise, L. d'Arcio, M. Dehne, G. Heinzel, H. Hogenhuis, M. Perreur-Lloyd, A. Taylor, and G. Wanner. Optical bench development for lisa. In Naoto Kadowaki, editor, *International Conference on Space Optics — ICSO 2010*. SPIE, November 2017.

[7] Shreevathsa Chalathadka Subrahmanya, Christian Darsow-Fromm, and Oliver Gerberding. Integrating high-precision and fringe-scale displacement sensing using heterodyne cavity-tracking. *Optics Express*, 33(3):4044, January 2025.

[8] M Chwalla, K Danzmann, G Fernández Barranco, E Fitzsimons, O Gerberding, G Heinzel, C J Killow, M Lieser, M Perreur-Lloyd, D I Robertson, S Schuster, T S Schwarze, M Tröbs, H Ward, and M Zwetz. Design and construction of an optical test bed for lisa imaging systems and tilt-to-length coupling. *Classical and Quantum Gravity*, 33(24):245015, November 2016.

[9] C. Corsi, I. Liontos, S. Cavalieri, M. Bellini, G. Venturi, and R. Eramo. An ultrastable michelson interferometer for high-resolution spectroscopy in the xuv. *Optics Express*, 23(4):4106, February 2015.

[10] Karsten Danzmann and Albrecht Ruediger. Lisa technology concept, status, prospects. *Classical and Quantum Gravity*, 20(10):S1–S9, April 2003.

[11] Marina Dehne. Construction and noise behaviour of ultra-stable optical systems for space interferometers. 2012.

[12] Johannes Eichholz, David B. Tanner, and Guido Mueller. Heterodyne laser frequency stabilization for long baseline optical interferometry in space-based gravitational wave detectors. *Phys. Rev. D*, 92:022004, Jul 2015.

[13] Roland Fleddermann, Christian Diekmann, Frank Steier, Michael Tröbs, Gerhard Heinzel, and Karsten Danzmann. Sub-pm$\sqrt{\mathrm{Hz}}^{-1}$ non-reciprocal noise in the lisa backlink fiber. *Classical and Quantum Gravity*, 35(7):075007, February 2018.

[14] Yungui Gong, Jun Luo, and Bin Wang. Concepts and status of chinese space gravitational wave detection projects. *Nature Astronomy*, 5(9):881–889, September 2021.

[15] Esa Jaatinen, David J Hopper, and Julian Back. Residual amplitude modulation mechanisms in modulation transfer spectroscopy that use electro-optic modulators. *Measurement Science and Technology*, 20(2):025302, December 2008.

[16] Kylan Jersey, Harold Hollis, Han-Yu Chia, Jose Sanjuan, Paul Fulda, Guido Mueller, and Felipe Guzman. Picometer sensitive prototype of the optical truss interferometer for lisa, 2024.

[17] J. B. Johnson. Thermal agitation of electricity in conductors. *Physical Review*, 32(1):97–109, July 1928.

[18] Seiji Kawamura, Masaki Ando, Naoki Seto, Shuichi Sato, Mitsuru Musha, Isao Kawano, Jun'ichi Yokoyama, Takahiro Tanaka, Kunihito Ioka, Tomotada Akutsu, Takeshi Takashima, Kazuhiro Agatsuma, Akito Araya, Naoki Aritomi, Hideki Asada, Takeshi Chiba, Satoshi Eguchi, Motohiro Enoki, Masa-Katsu Fujimoto, Ryuichi Fujita, Toshifumi Futamase, Tomohiro Harada, Kazuhiro Hayama, Yoshiaki Himemoto, Takashi Hiramatsu, Feng-Lei Hong, Mizuhiko Hosokawa, Kiyotomo Ichiki, Satoshi Ikari, Hideki Ishihara, Tomohiro Ishikawa, Yousuke Itoh, Takahiro Ito, Shoki Iwaguchi, Kiwamu Izumi, Nobuyuki Kanda, Shinya Kanemura, Fumiko Kawazoe, Shiho Kobayashi, Kazunori Kohri, Yasufumi Kojima, Keiko Kokeyama, Kei Kotake, Sachiko Kuroyanagi, Kei-ichi Maeda, Shuhei Matsushita, Yuta Michimura, Taigen Morimoto, Shinji Mukohyama, Koji Nagano, Shigeo Nagano, Takeo Naito, Kouji Nakamura, Takashi Nakamura, Hiroyuki Nakano, Kenichi Nakao, Shinichi Nakasuka, Yoshinori Nakayama, Kazuhiro Nakazawa, Atsushi Nishizawa, Masashi Ohkawa, Kenichi Oohara, Norichika Sago, Motoyuki Saijo, Masaaki Sakagami, Shin-ichiro Sakai, Takashi Sato, Masaru Shibata, Hisaaki Shinkai, Ayaka Shoda, Kentaro Somiya, Hajime Sotani, Ryutaro Takahashi, Hirotaka Takahashi, Takamori Akiteru,

Keisuke Taniguchi, Atsushi Taruya, Kimio Tsubono, Shinji Tsujikawa, Akitoshi Ueda, Ken-ichi Ueda, Izumi Watanabe, Kent Yagi, Rika Yamada, Shuichiro Yokoyama, Chul-Moon Yoo, and Zong-Hong Zhu. Current status of space gravitational wave antenna decigo and b-decigo. *Progress of Theoretical and Experimental Physics*, 2021(5), February 2021.

[19] Keiko Kokeyama, Kiwamu Izumi, William Z. Korth, Nicolas Smith-Lefebvre, Koji Arai, and Rana X. Adhikari. Residual amplitude modulation in interferometric gravitational wave detectors. *Journal of the Optical Society of America A*, 31(1):81, December 2013.

[20] W Z Korth, A Heptonstall, E D Hall, K Arai, E K Gustafson, and R X Adhikari. Passive, free-space heterodyne laser gyroscope. *Classical and Quantum Gravity*, 33(3):035004, January 2016.

[21] W Z Korth, A Heptonstall, E D Hall, K Arai, E K Gustafson, and R X Adhikari. Passive, free-space heterodyne laser gyroscope. *Classical and Quantum Gravity*, 33(3):035004, January 2016.

[22] Soham Kulkarni, Ada Umińska, Joseph Gleason, Simon Barke, Reid Ferguson, Jose Sanjuán, Paul Fulda, and Guido Mueller. Ultrastable optical components using adjustable commercial mirror mounts anchored in a ule spacer. *Applied Optics*, 59(23):6999, August 2020.

[23] Alexey Kupriyanov, Arthur Reis, Annike Knabe, Nina Fletling, Alireza HosseiniArani, Mohsen Romeshkani, Manuel Schilling, Vitali Müller, and Jürgen Müller. *Analysis of Novel Sensors and Satellite Formation Flights for Future Gravimetry Missions*. Springer Berlin Heidelberg, 2024.

[24] Jun Luo, Li-Sheng Chen, Hui-Zong Duan, Yun-Gui Gong, Shoucun Hu, Jianghui Ji, Qi Liu, Jianwei Mei, Vadim Milyukov, Mikhail Sazhin, Cheng-Gang Shao, Viktor T Toth, Hai-Bo Tu, Yamin Wang, Yan Wang, Hsien-Chi Yeh, Ming-Sheng Zhan, Yonghe Zhang, Vladimir Zharov, and Ze-Bing Zhou. Tianqin: a space-borne gravitational wave detector. *Classical and Quantum Gravity*, 33(3):035010, January 2016.

[25] Sizuo Luo, Robin Weissenbilder, Hugo Laurell, Mattias Ammitzböll, Vénus Poulain, David Busto, Lana Neoričić, Chen Guo, Shiyang Zhong, David Kroon, Richard J Squibb, Raimund Feifel, Mathieu Gisselbrecht, Anne L'Huillier, and Cord L Arnold. Ultra-stable and versatile high-energy resolution setup for attosecond photoelectron spectroscopy. *Advances in Physics: X*, 8(1), September 2023.

[26] Pavla Nekvindová, Jarmila Špirková, Jarmila Červená, Milos Budnar, Alenka Razpet, Benjamin Zorko, and Primož Pelicon. Annealed proton exchanged optical waveguides in lithium niobate: differences between the x- and z-cuts. *Optical Materials*, 19(2):245–253, April 2002.

[27] Newport. Suprema® zerodrift™ thermally compensated mirror mounts - su100tw-f2k. Technical report, Spectra-Physics GmbH, 2020.

[28] H. Nyquist. Thermal agitation of electric charge in conductors. *Physical Review*, 32(1):110–113, July 1928.

[29] M. Diaz Ortiz, J. Gleason, H. Grote, A. Hallal, M. T. Hartman, H. Hollis, K. S. Isleif, A. James, K. Karan, T. Kozlowski, A. Lindner, G. Messineo, G. Mueller, J. H. Poeld, R. C. G. Smith, A. D. Spector, D. B. Tanner, L. W. Wei, and B. Willke. Design of the alps ii optical system, 2020.

[30] D I Robertson, E D Fitzsimons, C J Killow, M Perreur-Lloyd, H Ward, J Bryant, A M Cruise, G Dixon, D Hoyland, D Smith, and J Bogenstahl. Construction and testing of the optical bench for lisa pathfinder. *Classical and Quantum Gravity*, 30(8):085006, March 2013.

[31] David Roma-Dollase, Vivek Gualani, Martin Gohlke, Klaus Abich, Jordan Morales, Alba Gonzalvez, Victor Martín, Juan Ramos-Castro, Josep Sanjuan, and Miquel Nofrarias. Resistive-based micro-kelvin temperature resolution for ultra-stable space experiments. *Sensors*, 23(1):145, December 2022.

[32] J. Sanjuán, A. Lobo, M. Nofrarias, J. Ramos-Castro, and P. J. Riu. Thermal diagnostics front-end electronics for lisa pathfinder. *Review of Scientific Instruments*, 78(10), October 2007.

[33] C P Sasso, G Mana, and S Mottini. The lisa interferometer: impact of stray light on the phase of

the heterodyne signal. *Classical and Quantum Gravity*, 36(7):075015, March 2019.

[34] Etienne Savalle, Aurélien Hees, Florian Frank, Etienne Cantin, Paul-Eric Pottie, Benjamin M. Roberts, Lucie Cros, Ben T. McAllister, and Peter Wolf. Searching for dark matter with an optical cavity and an unequal-delay interferometer. *Phys. Rev. Lett.*, 126:051301, Feb 2021.

[35] B. S. Sheard, G. Heinzel, K. Danzmann, D. A. Shaddock, W. M. Klipstein, and W. M. Folkner. Intersatellite laser ranging instrument for the grace follow-on mission. *Journal of Geodesy*, 86(12):1083–1095, May 2012.

[36] F Steier, R Fleddermann, J Bogenstahl, C Diekmann, G Heinzel, and K Danzmann. Construction of the lisa back-side fibre link interferometer prototype. *Classical and Quantum Gravity*, 26(17):175016, August 2009.

[37] Michael Tröbs. Laser development and stabilization for the spaceborne interferometric gravitational wave detector lisa. 2005.

[38] Michael Tröbs and Gerhard Heinzel. Improved spectrum estimation from digitized time series on a logarithmic frequency axis. *Measurement*, 39(2):120–129, February 2006.